Article

N-Alkyl Interstitial Spacers and Terminal Pendants Influence the Alkaline Stability of Tetraalkylammonium Cations for Anion Exchange Membrane Fuel Cells

Sean A. Nunez, Clara Capparelli, and Michael A. Hickner

Chem. Mater., **Just Accepted Manuscript** • DOI: 10.1021/acs.chemmater.5b04767 • Publication Date (Web): 03 Mar 2016

N-Alkyl Interstitial Spacers and Terminal Pendants Influence the Alkaline Stability of Tetraalkylammonium Cations for Anion Exchange Membrane Fuel Cells

Sean A. Nuñez, Clara Capparelli, and Michael A. Hickner*

Department of Materials Science and Engineering, The Pennsylvania State University, University Park, Pennsylvania 16802, United States

ABSTRACT: Current performance targets for anion-exchange membrane (AEM) fuel cells call for greater than 95% alkaline stability for 5000 hours at temperatures up to 120 °C. Using this target temperature of 120 °C, we provide an incisive ^{1}H NMR-based alkaline degradation method to identify the degradation products of n-alkyl spacer tetraalkylammonium cations in various AEM polymers and small molecule analogs. The operative alkaline degradation mechanisms and rates on benzyltrimethylammonium-, n-alkyl interstitial spacer- and n-alkyl terminal pendant-cations are compared in several architectures. Our findings indicate that benzyltrimethylammonium- and n-alkyl terminal pendant cations are significantly more labile than an n-alkyl interstitial spacer-cation. Additionally, we found that the alkaline stability of an n-alkyl interstitial spacer cation is enhanced when combined with an n-alkyl terminal pendant. At 120 °C, an inverse trend was observed in the overall stability of AEM poly(styrene) and AEM poly(phenylene oxide) samples compared to what has been shown at 80 °C. Follow-up small molecule studies suggest that at 120 °C, a 1,4-elimination degradation mechanism may be activated on styrenic AEM polymers capable of forming hyperconjugated resonance hybrids.

INTRODUCTION

The global demand for energy is projected to rise 1.8% YOY until 2020 with an expected fossil fuel consumption growth of only 0.8% YOY.[1] This discrepancy between growing demand and fossil fuel supply increase has driven the development of alternative energy technologies that utilize renewable materials and employ renewable- and regeneration-schemes bearing low environment impact. Fuel cells rely on renewable feedstocks for the electrochemical conversion of renewable fuels to electrical energy for primary power applications and energy storage systems. Anion exchange membrane (AEM) fuel cells have been proposed as viable alternatives to proton exchange membrane fuel cells (PEMFCs)[2–4] arising from their use of platinum-free electrodes.[5-7] Additionally, AEMs may be useful in electrolyzers[7] that feature precious metal-free catalysts.[8-10] The low cost of non-precious metal catalysts is the clear motivator for AEM-based devices, and these types of cells also have increased tolerance to CO[11] or NH_3[12] impurities in the fuel which can extend their applicability significantly over PEM-based devices. In early work, AEM devices showed low polarization performance, but new AEMs have conductivities that rival PEMs.[13,14] However, the use of AEMs in a wide range of devices has been limited due to the polymers' poor stability in the highly alkaline electrochemical environment within fuel cells that require the generation of hydroxide anions and transport through the solid polymer membrane. Consequently, at higher temperatures, the alkaline stability of AEM polymer backbones and cations poses a significant challenge for developing AEM fuel cell devices capable of achieving the Department of Energy's 2015 performance targets calling for greater than 95% alkaline stability for 5000 hours at temperature up to 120 °C.[15]

Polymer-bound cations for use in AEMs have included benzimidazolium,[16] imidazolium,[14,17,18] amino phosphonium[19] and sulfonium,[20] but the most commonly studied cations are tetraalkylammonium (TAA) salts due to their synthetic accessibility, inexpensive starting materials, and verified practical membrane properties. TAA cations have demonstrated appreciable alkaline stability, but remain susceptible to a variety of chemical degradation pathways. These degradation mechanisms include substitutions (S_N2),[21,22] eliminations (E2),[22,23] Stevens or Sommelet—Hauser rearrangements[23] and potentially, anion-induced 1,4-eliminations[14] (Figure 1).

Several studies[24,25] on polymer-bound TAA cations have substantiated the occurrence of substitution reactions,[26,27] but the contribution of Hofmann eliminations remains a matter of discussion with little experimental evidence in AEM polymers. Stevens and Sommelet—Hauser rearrangements on benzyltrimethylammonium (BTMA) cations have been demonstrated under alkaline aqueous conditions[28] and *in silico*,[29,30] but have not been experimentally observed in AEM materials.[24] A possible explanation for this result may involve side reactions in the presence of nucleophilic counterions.[28]

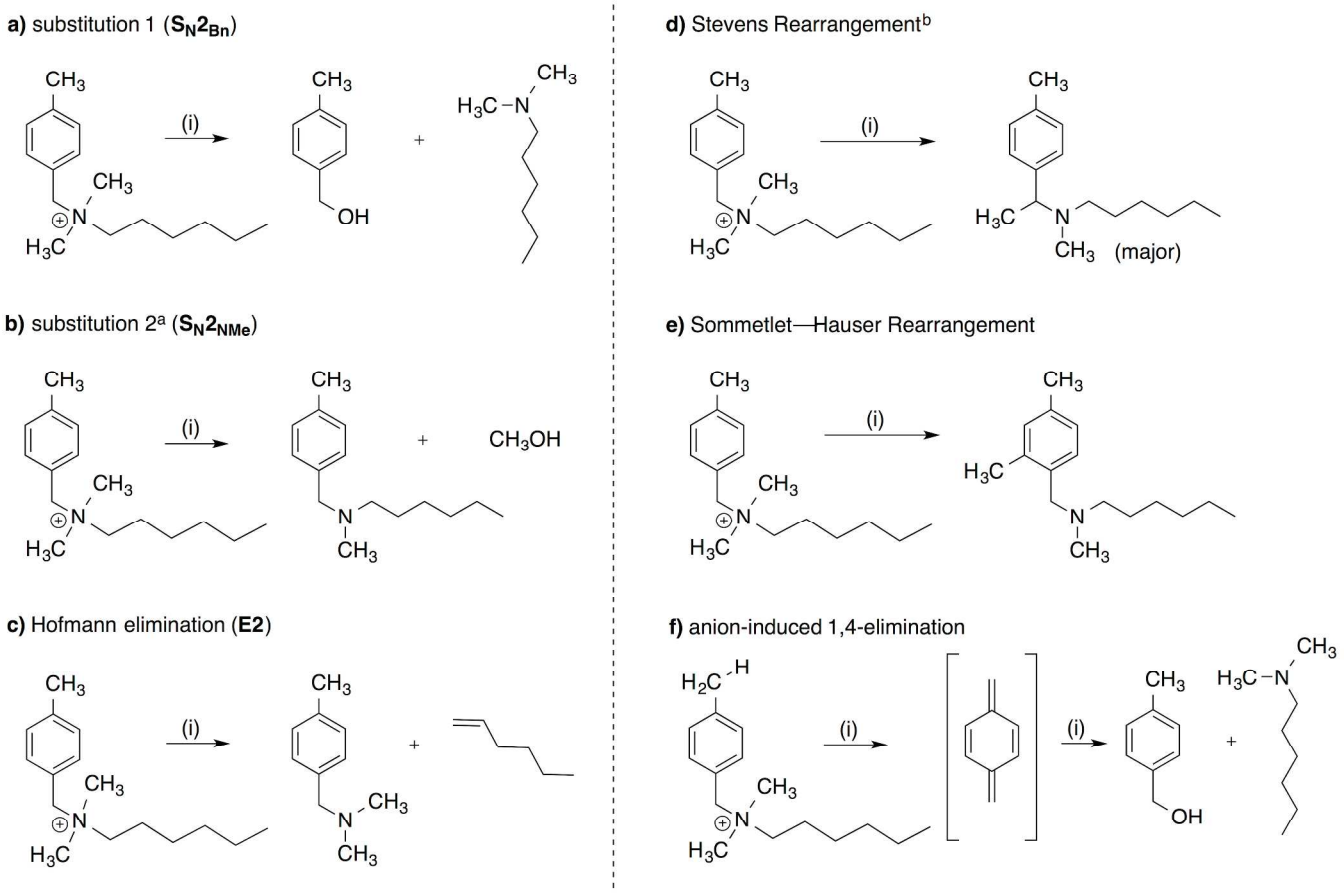

Figure 1. Chemical degradation reaction mechanisms for a TAA small molecule under (i) alkaline aqueous conditions. [a]A minor product of this substitution reaction results in 1-hexanol (not shown) as the dealkylation product.[31] [b]A minor product of the Steven's rearrangement results in the [2,3]-shift product (not shown).[30] Anion-induced 1,4-eliminations (f) arise from the presence of an acidic hydrogen paired with a good leaving group (e.g., TAA cation) in the highlighted configuration to generate a transient 1,4-quinodimethane intermediate that hydrolyses under aqueous conditions.

Finally, anion-induced 1,4-eliminations, a degradation mechanism (seldom discussed in the context of AEM degradation) is fundamentally allowed when BTMA analogues (e.g., a TAA functionalized polystyrene) contain an acidic hydrogen in ring-activated positions that is electronically paired with a leaving group (Figure 1f).[32] Unfortunately, the contribution of 1,4-eliminations cannot easily be discerned from benzyl substitutions under aqueous alkaline degradation conditions without sophisticated isotopic labeling studies and full analysis of the degradation products.[33]

A recent review by Kreuer argued that *claims about base stable* [TAA cations] *are abundant, but so far, many results have not been verified by independent studies*.[34] In addition, Kreuer surmised that the steric shielding of cations with (alkyl) spacers offers the most promising approach to increase alkaline stability, which is likely the result of increasing hydrophobicity or steric hindrance around the cationic center.[35] Indeed these claims of enhanced alkaline stability have been corroborated in AEM polymers with the implementation of: (i) *interstitial n*-alkyl spacers between the polymer backbone and nitrogen of the TAA,[36,37] (ii) *terminal n*-alkyl pendants from the nitrogen of the TAA,[38] and (iii) crosslinking spacers adjoining TAA groups from two congruent polymer backbones.[39,40]

Given the synthetic challenges of simple and effective post-polymerization chemical modifications to incorporate interstitial *n*-alkyl spacers, most attempts at increased stability of TAA-based AEM polymers feature diamine crosslinkers or terminal alkyl chains. Diamine crosslinkers and terminal spacers, while sterically shielding, generally contain *β*-hydrogen(s) that may introduce the potential for Hofmann eliminations. Interestingly, the specific contribution of Hofmann eliminations to polymer-bound TAA cations, contrary to many claims, has not been directly substantiated or compared to the relative contributions of other possible degradation mechanisms. Therefore, incisive chemical methods that provide robust identification of reaction products bound to the polymer chain and in the degradation solutions are required for measuring the degradation products, rates, and resulting changes to the polymer structure with the aim of designing robust AEM polymers.

Our prior work[26] has: (i) highlighted the utility of small molecule analogs for the study of AEM polymer degradation, (ii) demonstrated a spectroscopic method to systematically measure AEM alkaline stability under controlled and reproducible test conditions, and (iii) substantiated the contribution of polymer backbones on alkaline stability. Furthermore, an emphasis was placed on *the importance of ranking alkaline stability under harsh conditions where degradation is clearly observed*. The given suggestion was that degradation could not be readily assessed unless there is significant reaction or conversion of the polymer or small molecule.

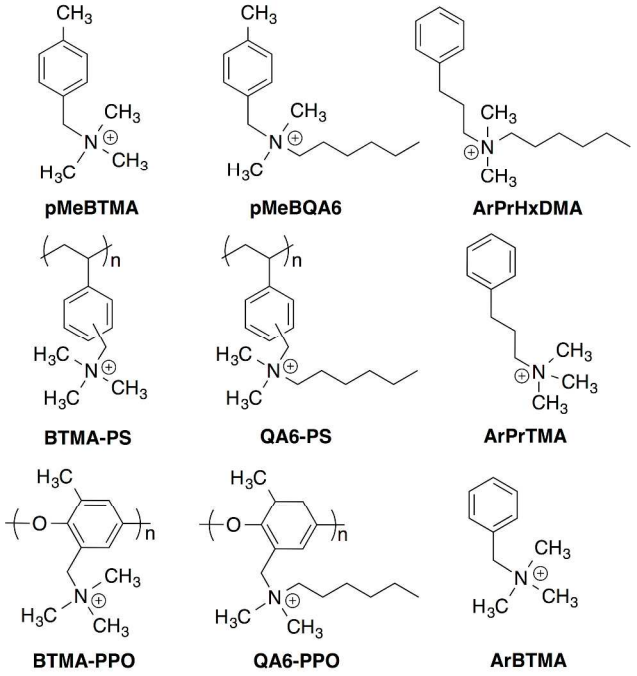

Figure 2. Chemical structures of TAA small molecule AEM analogs and polymers studied.

The AEM literature often claims good stability at low temperatures (e.g., 60 °C) while often reporting poor device stability. This contradiction identifies a clear disconnect between membrane and device studies. To consolidate these issues, follow-up studies have focused on methods that are specifically designed to cause the degradation of both the polymer backbone and TAA cation architectures to identify leads for advanced synthetic designs. Raising the temperatures in excess of 80 °C is needed to assess the intrinsic stability of AEM structures. Additionally, lowering the dielectric constant of the degradation medium appears to be critical in observing functional group degradation in a reasonable time period.[38,39]

Herein, a comparison between the relative alkaline stability and operative degradation mechanisms in BTMA- and various TAA samples are determined by ^{1}H NMR at 120 °C in the presence of excess NaOD in a 3:1 solution of CD_3OD–D_2O. Three BTMA-functionalized compounds consisting of **pMeBTMA**, **BTMA-PS**, and **BTMA-PPO** (Figure 2) were evaluated. Additionally we examined compounds containing n-alkyl terminal spacers of variable length: **pMeBQA6**, **QA6-PS**, and **QA6-PPO**. Finally, we studied the degradation of **ArPrTMA** as a small molecule analog containing an interstitial spacer and **ArPrHxDMA** that contains both an interstitial and terminal spacer. The approach presented offers mechanistic insight into the contribution of the polymer backbones to the stability of these materials and the effect of n-alkyl spacers on the degradation of TAA-based cations.

EXPERIMENTAL

Materials

All reactions were performed in flame-dried glassware under positive pressure of nitrogen, unless otherwise noted. Air- and moisture-sensitive liquids were transferred by syringe or cannula. Organic solutions were concentrated by rotary evaporation (1–20 mmHg) at ambient temperature, unless otherwise noted. Poly(2,6-dimethyl-1,4-phenylene oxide) (Aldrich), poly(styrene-co-chloromethylstyrene) (Aldrich), benzyltrimethylammonium chloride (≥98.0%,), CD_3OD (D, 99.8%) and D_2O (D, 99.9%) (Cambridge Isotope Laboratories), sodium deuteroxide (40 wt. % in D_2O, D, 99.5%), 1,4-dioxane (anhydrous, 99.8%, Aldrich), 1-hexene (97%, Aldrich), trimethylamine (~45 wt. % in H_2O, Aldrich), 4-methylbenzyl alcohol (98%, Aldrich), 1-hexanol (98%, Aldrich), benzyl alcohol (99%, Alfa Aesar), 3-phenyl-1-propanol (98%, TCI), *N*,*N*-dimethylbenzylamine (≥99%, Aldrich), and all other reagents were purchased commercially and were used as received unless otherwise noted. Thin-layer chromatography was carried out on Dynamic Adsorbents silica gel TLC (20 × 20 w/h, F-254, 250 μm). Deionized water was purified with a Millipore purification system (Milli–Q UV Plus). High temperature NMR samples were prepared in Wilmad quick pressure valve tubes (5 mm, heavy wall, 300 MHz or better).

Instrumentation

Proton nuclear magnetic resonance (^{1}H NMR) spectra were obtained on a Bruker DPX-300. ^{1}H NMR spectra of non-degradation samples were recorded at 25 °C unless otherwise specified. Proton chemical shifts are expressed in parts per million (ppm, δ scale), and are referenced to tetramethylsilane ($(CH_3)_4Si$, 0.00 ppm) or to residual protium in the solvent ($CHCl_3$, 7.27 ppm; CD_2HOD, 3.31 ppm; CD_3SOCD_2H, 2.50 ppm) or to an internal standard (1,4-dioxane, 3.70 ppm). Data are represented as follows: chemical shift, multiplicity (s = singlet, d = doublet, t = triplet, q = quartet, m = multiplet and/or multiple resonances), integration, and coupling constant (*J*) in hertz.

Processing

Acquisition data was processed using Bruker Topspin 3.2 software. Sample peak areas were assigned based on standards and further normalized to the peak area of the internal standard. Stacked overlay visualizations are scaled to their normalized peak area values.

General Procedure for Sample Preparation and Data Acquisition.

To a **BTMA–PS** sample (15.8 mg) was added CD_3OD (1875 μL), D_2O (429.5 μL) and a 1.8 M solution of 1,4-dioxane (internal standard) in D_2O (41.5 μL). The vial was capped and vortexed until the polymer was completely dissolved (□60 s). To the resulting solution was added a 40% wt/v solution of NaOD in D_2O (140 μL), and the vial was recapped and briefly vortexed (□5 s). The solution was evenly divided into two heavy-wall NMR tubes (300 MHz, 5 mm, 7 in., max. pressure 205 psi) and fitted with a PTFE screw cap. The sample placed in a ceramic collar and inserted into a 300 MHz NMR spectrometer equipped with a variable-temperature probe preheated to 60 °C. The sample was allowed to equilibrate (~5 min) and the spectrometer programed to acquire an initial spectrum with 48 scans and a relaxation time of 5 s. Upon completion of the acquisition, the sample NMR tube was removed from the spectrometer and inserted into a solid-state aluminum heating block preheated to 120 °C (see SI for specifications). After each consecutive hour, the sample tube was removed from the heating block, agitated by inversion (2 ×) and inserted into the

spectrometer for additional acquisitions using identical parameters to the initial spectrum.

Synthesis

pMeBTMA. To a round-bottom flask was added 4-methylbenzylbromide (1.0 g, 5.4 mmol, 1 equiv.) and tetrahydrofuran (5 mL). The flask was cooled to 0 °C and an aqueous solution of trimethylamine (~45 wt. %, 5 mL) was added. The flask was warmed to 25 °C and was stirred for 12 h. The excess trimethylamine was removed by bubbling nitrogen gas through the product mixture for 3 h at 25 °C. The product mixture was then concentrated under reduced pressure (0.1 torr) at 25 °C for 24 h to afford **pMeBTMA** as a white powder. ^{1}H NMR (CD_3OD): δ 7.53 (d, 2H, J = 8.1 Hz), 7.34 (d, 2H, J = 7.7 Hz), 4.64 (s, 2H), 3.14–3.17 (s, 9H), 2.39 (s, 3H).

pMeBQA6. To a round-bottom flask equipped with a stir bar was added 4-methylbenzylbromide (1.0 equiv., 1.35 mmol, 250 mg), N,N-dimethylhexylamine (1.0 equiv., 1.35 mmol, 0.45 mL) and THF (1.35 mL). The flask was sealed and stirred for 24 h at 25 °C. The residual solvent was evaporated from the crude product mixture under reduced pressure followed by the addition of ethyl acetate (10 mL) and the organics were washed with 0.1 M HCl (2 × 10 mL). The organics were washed with deionized water (2 × 10 mL) and the organics collected and dried over sodium sulfate and evaporated under reduced. The product residue was then further dried under reduced pressure (0.1 torr) at 25 °C for 24 h to afford the chloride salt of **pMeBQA6** as a clear viscous liquid. ^{1}H NMR (CD_3OD): δ 7.43 (d, 2H, J = 10.8), 7.34 (d, 2H, J = 7.2), 4.50 (s, 2H), 3.28 (m, 2H), 3.02 (s, 6H), 2.41 (s, 3H), 1.86 (m, 2H), 1.40 (m, 6H), 0.93 (t, 3H, J = 7.2).

BTMA-PS. To a round-bottom flask was added poly(styrene-co-chloromethylstyrene) (2.0 g), tetrahydrofuran (10 mL), and an aqueous solution of trimethylamine (~45 wt. %, 10 mL). The flask was sealed and was stirred for 24 h at 25 °C. The excess trimethylamine was removed by bubbling nitrogen gas through the product mixture for 3 h at 25 °C. The product mixture was then concentrated under reduced pressure (0.1 torr) at 25 °C for 24 h to afford the chloride salt of **BTMA-PS** as a white translucent film. ^{1}H NMR (CD_3OD): δ 6.56–7.20 (m), 4.56 (br s), 3.05 (br s), 1.0–2.5 (m).

BTMA-PPO. To a round-bottom flask was added poly(2,6-dimethyl-1,4-phenylene oxide) (15 g, 125 mmol) and chlorobenzene (120 mL, 1.04 M) until the polymer was completely dissolved. To the flask was added N-bromosuccinimide (11.1 g, 62.5 mmol) and 2,2'-azobis-isobutyronitrile (0.63 g, 3.75 mmol). The flask was fitted with a reflux condenser and heated to 125 °C for 3 h. The product mixture was cooled to 25 °C and slowly poured into a flask of stirring ethanol (~1 L) at room temperature to precipitate the product residue. The product residue was filtered and washed with ethanol (2 × 200 mL). The product residue was collected and dissolved in chloroform (150 mL) and then reprecipitated in ethanol (~1 L). The product was collected and dried under reduced pressure (0.1 torr) for 12 h to afford a yellow powder. The aforementioned yellow powder precursor (2.0 g) was added to a round-bottom flask to the flask was added *N,N*-dimethylacetamide (10 mL) and an aqueous solution of trimethylamine (~45 wt. %, 10 mL). The flask was sealed and was stirred for 24 h at 25 °C. Excess trimethylamine was removed by bubbling nitrogen gas through the product mixture for 3 h at 25 °C. The product mixture was poured into a recrystillization dish and the solvent removed in a vacuum (~1 torr) oven at 35 °C. The resulting brittle film was removed to afford **BTMA-PPO** as yellow powder. ^{1}H NMR ($CDCl_3$): δ 6.63–6.70 (m), 6.46–6.51 (m), 4.33 (s), 2.08 (s).

QA6-PPO. To a round bottom flask equipped with a stir bar was added poly(styrene-co-chloromethylstyrene) (1.0 equiv., 14.2 mmol, 2.0 g), dimethylacetamide (20 mL), deionized water (4 mL), and N,N-dimethylhexylamine (2.5 equiv., 35.5 mmol, 6.1 mL). The flask was sealed and stirred for 24 h at 25 °C. To the product mixture was added diethyl ether (40 mL) and the organics washed with 0.1 M HCl (3 × 40 mL). The organics were then washed with deionized water (2 × 20 mL) and the organics collected and dried over sodium sulfate and evaporated under reduced. The product residue was then further dried under reduced pressure (0.1 torr) at 25 °C for 24 h to afford the chloride salt of **QA6-PPO** as a tacky yellow crystalline solid. ^{1}H NMR (DMSO-d_6): δ 6.50–6.97 (bm, 2H), 4.36 (bs, 2H), 3.17 (bm, 2H), 2.96 (bs, 6H), 2.02 (bm, 2H), 1.62 (bm, 2H), 1.21 (bm, 6H), 0.80 (bs, 3H).

ArPrHxDMA. To a round bottom flask equipped with a magnetic stir bar was added 1-bromo-3-phenylpropane (1.0 equiv., 13.2 mmol, 2.0 mL), tetrahydrofuran (10 mL), and N,N-dimethylhexylamine (3.0 equiv., 39.4 mmol, 6.85 mL). The flask was sealed and stirred for for 24 h at 25 °C. The residual solvent was evaporated from the crude product mixture under reduced pressure followed by the addition of ethyl acetate (10 mL) and the organics were washed with 0.1 M HCl (2 × 10 mL). The organics were washed with deionized water (2 × 10 mL) and the organics collected and dried over sodium sulfate and evaporated under reduced. The product residue was then further dried under reduced pressure (0.1 torr) at 25 °C for 24 h to afford the chloride salt of **ArPrHxDMA** as white foam. ^{1}H NMR (CD_3OD:D_2O (3:1)): δ 7.27–7.31 (m, 5H), 3.05 (s, 6H), 2.71 (m, 2H), 2.06 (m, 2H), 1.64 (m, 2H), 1.34 (m, 6H), 0.93 (t, 3H).

QA6-PS. To a round-bottom flask was added poly(styrene-co-chloromethylstyrene) (2.0 g), dimethylacetamide (20 mL), deionized water (4 mL), and N,N-dimethylhexylamine (5.0 equiv., 71 mmol, 12.3 mL). The flask was sealed and was stirred for 24 h at 25 °C. To the product mixture was added diethyl ether (40 mL) and the organics washed with 0.1 M HCl (3 × 40 mL). The organics were then washed with deionized water (2 × 20 mL) and the organics collected and dried over sodium sulfate and evaporated under reduced pressure. The product residue was then further dried under reduced pressure (0.1 torr) at 25 °C for 24 h to afford the chloride salt of QA6-PS as a white foam. ^{1}H NMR (CD_3OD:D_2O (3:1)): δ 6.47–7.22 (bm, 4H), 4.53 (bs, 2H), 3.26 (bm, 2H), 2.86 (bs, 6H), 1.76 (bm, 2H), 1.27 (bm, 6H), 0.85 (bm, 3H).

ArPrTMA. To a round bottom flask equipped with a magnetic stir bar was added 1-bromo-3-phenylpropane (1.0 equiv., 13.2 mmol, 2.0 mL), tetrahydrofuran (10 mL).

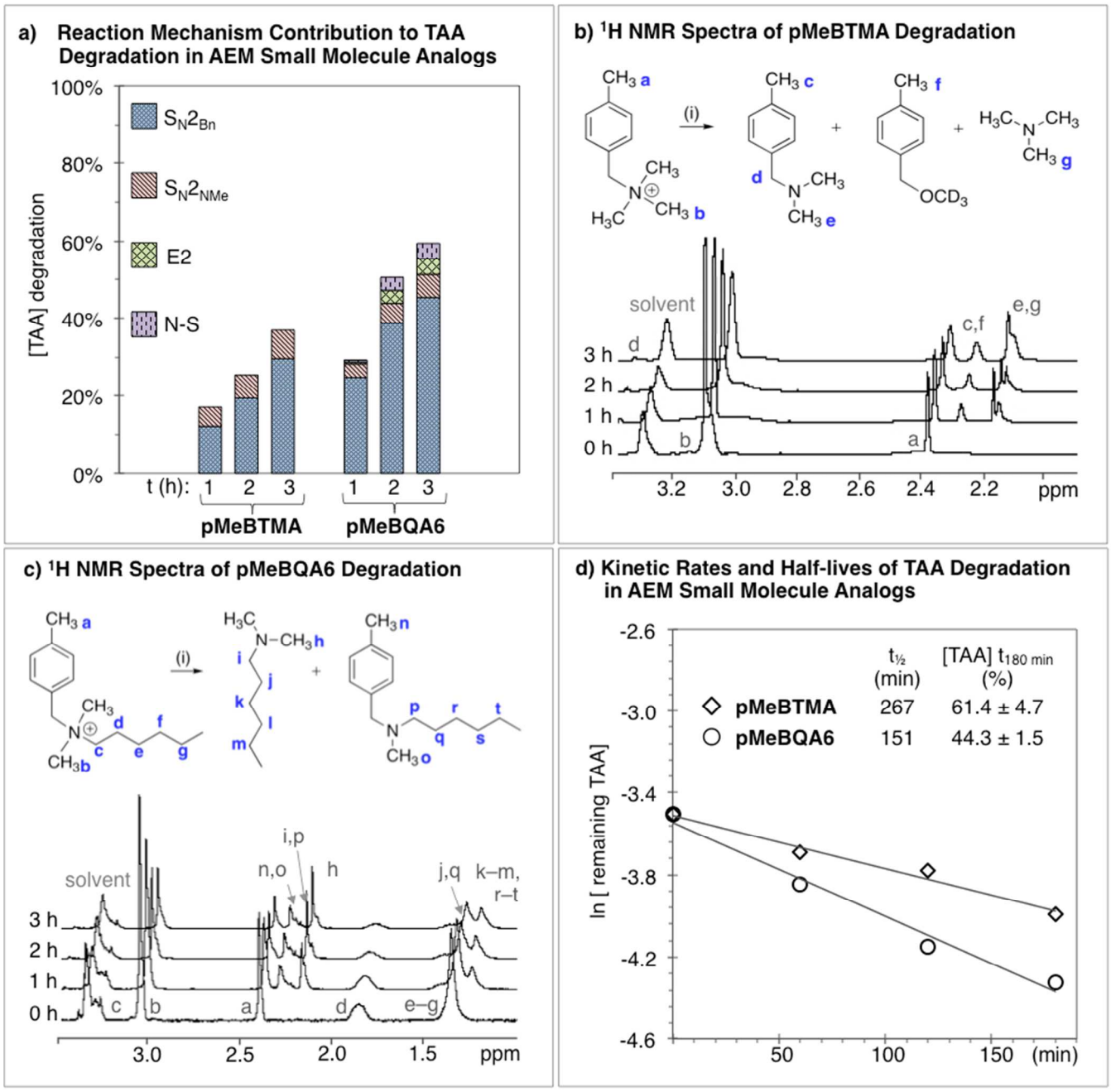

Figure 3. Rates of degradation and offset ^{1}H NMR spectral overlays of **pMeBTMA** and **pMeBQA6** as (i) 30 mM solutions in CD_3OD–D_2O (3:1), 1,4–dioxane (int. std.), and NaOD (20 equiv., 0.6 M) from 0–3 h shown in hourly intervals at 120 °C. QA-PPO displayed turbidity at 3 h hours and was not included in our analyses. Mechanism abbreviations are benzyl substitution (S_N2_{Bn}), dealkylation (S_N2_{NMe}), Hofmann elimination (E2), non-specific (N–S); the difference in decay between the TAA cation and the sum of observed byproducts.

The flask was cooled to 0 °C and an aqueous solution of trimethylamine (~45 wt. %, 5 mL) was added. The flask was warmed to 25 °C and was stirred for 24 h. The excess trimethylamine was removed by bubbling nitrogen gas through the product mixture for 3 h at 25 °C. The product mixture was then concentrated under reduced pressure (0.1 torr) at 25 °C for 24 h to afford **ArPrTMA** as a white foam. ^{1}H NMR (CD_3OD:D_2O (3:1)): δ 7.24–7.35 (m, 5H), 3.36 (m, 2H), 3.15 (s, 9H), 2.78 (m, 2H), 2.18 (m, 2H).

RESULTS AND DISCUSSION

The products resulting from the degradation of TAA cations are extensive but were simplified by considering only the degradation products that were most likely to occur. For instance, the absence of *β*-hydrogens for benzyltrimethylammonium samples analyzed precludes Hofmann eliminations (E2). Likewise, the presence of an interstitial spacer limits the possibility of Sommelet–Hauser and Stevens rearrangements in **ArPrHxDMA**. Equally important is the inability to distinguish between anion-induced 1,4-eliminations (in all samples excluding PPO where this mechanism is not possible) and benzyl substitution.

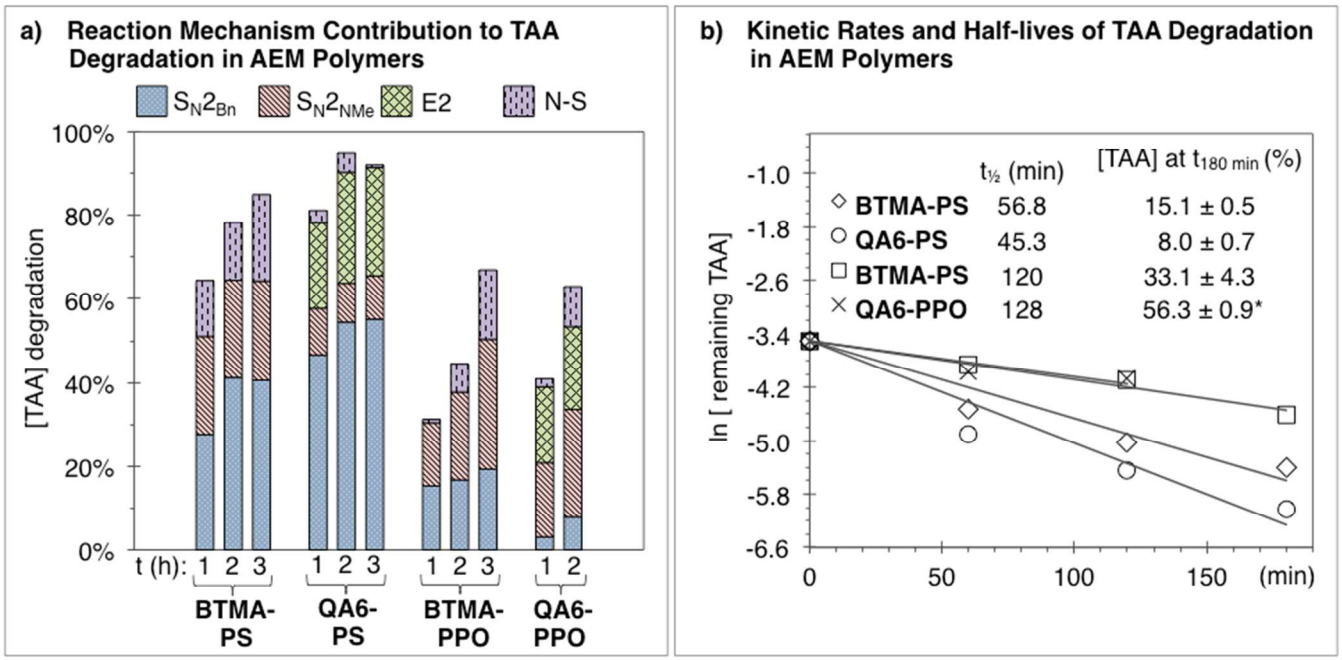

Figure 4. (a) Degradation rates and (b) degradation kinetics for **BTMA-PS**, **QA6-PS**, **BTMA-PPO**, and **QA6-PPO** as 30 mM solutions in CD_3OD–D_2O (3:1), 1,4–dioxane (int. std.), and NaOD (20 equiv., 0.6 M) from 0–3 h shown in hourly intervals at 120 °C. Mechanisms depicted are benzyl substitution (S_N2_{Bn}), dealkylation (S_N2_{NMe}), Hofmann elimination (E2), non-specific (N–S).

For this reason, the shared products of these degradation pathways were strictly treated as substitution (S_N2_{Bn} or S_N2_{NMe}) at the benzyl position.

Any decay of starting TAA spectral peaks without corresponding products of degradation were categorized as *non-specific* (N-S) degradation. Additionally, in selected experiments precipitation and/or turbidity resulted during the heating process (e.g., QA6-PPO). In such instances, an analysis was conducted only on spectra wherein the sample remained soluble.

To aid in the interpretation of our results, we conducted small molecule ^{1}H NMR reference experiments on standards under analogous alkaline solution conditions. These standards consisted of commercially-available or synthesized small molecule analogs of the major degradation products. However in some cases, where ^{1}H NMR spectral analyses discerned only one byproduct of a specific degradation pathway due to overlapping peaks, the discernable mechanism-specific product was used for the determination of the operative degradation mechanism.

Influence of Terminal N-Alkyl Pendants on Benzyl-Linked Cations

The incorporation of terminal n-alkyl pendants in TAAs has been identified as a facile route to achieve alkaline stability in cast AEMs.[38] In solution studies on small molecules and polymers, we observed that pendant n-alkyl chains *decreased* the stability of benzyldimethyl n-alkyl ammonium groups compared to BTMA analogs. Shown in Figure 3a is the contribution of each degradation mechanism to the overall degradation of the TAA group in **pMeBTMA** and **pMeBQA6** in a solution of 3:1 CD_3OD–D_2O with 20 equivalents of NaOD at 120 °C.

The progressive summation of the degradation of the initial compound indicates that benzyl substitution (S_N2_{Bn}) is the operative mechanism in both samples followed by dealkylation (S_N2_{NMe}) to a much lesser extent. Interestingly, the presence of Hofmann elimination (E2) in **pMeBQA6** is nearly insignificant (t = 3 h, 4.0%). Degradation was assessed using the aliphatic ^{1}H NMR regions displaying the characteristic products of degradation consisting of trimethylamine, p-methyl-N,N-dimethylbenzylamine, and p- methylbenzyl alcohol for **pMeBTMA** (Figure 3b) and N,N-dimethylhexylamine, and p-methyl-N-methyl-N-hexylbenzylamine for **pMeBQA6** (Figure 3c). The occurrence of Hofmann elimination was determined by the unsaturated protium of 1-hexene (not shown).

The comparison between **pMeBTMA** and **pMeBQA6** small molecules was designed to approximate the degradation kinetics and product distribution of their respective poly(styrene) macromolecules. **pMeBTMA** displayed a reduced loss of the TAA concentration (38.6% loss) compared to 55.7% loss of TAA for **pMeBQA6** at 3 h (Figure 3a) with both samples experiencing similar degradation from benzyl substitution (S_N2_{Bn}) and dealkylation (S_N2_{NMe}). Furthermore, the degradation product distributions for **pMeBTMA** indicated by H_f (2.25–2.33 ppm) and H_g (2.11–2.25 ppm) (Figure 3b), suggests the increase in degradation of **pMeBQA6** does not result from Hofmann elimination. Figure 3d shows the kinetic profiles of **pMeBTMA** and **pMeBQA6** with half lives of 267 min and 151 min, respectively, a significantly reduction over studies conducted at 80 °C.

The comparative degradation between our dissolved **pMeBTMA** and **pMeBQA6** samples were contrary to the increased stability of immersed solid membrane samples reported reported by Li, et al. in poly(phenylene oxides) (PPO) with terminal n-alkyl pendants,[43] and Pan, et al. with backbone-appended alkyl chains.[44] In those membrane studies, reduced solvation and tertiary structural effects (e.g., phase separation) limit interactions of the tetraalkylammonium cation with the surrounding alkaline media thus promoting stability in n-alkylated pendant functionalized AEMs in the solid state.

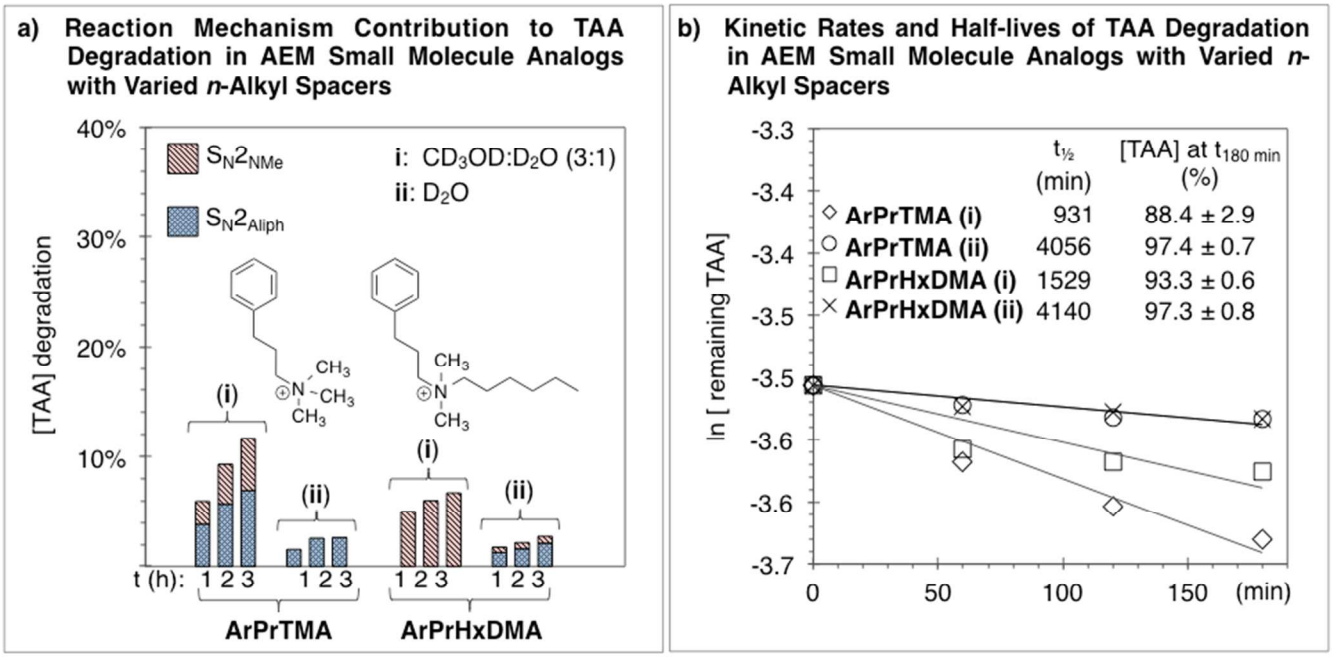

Figure 5. (a) Degradation rates for **ArPrTMA** and **ArPrHxDMA** as 30 mM solutions in either CD_3OD–D_2O (3:1) (i) or D_2O (ii), 1,4–dioxane (int. std.), and NaOD (20 equiv., 0.6 M) from 0–3 h shown in hourly intervals at 120 °C. (b) Degradation kinetics and half lives for **ArPrTMA** and **ArPrHxDMA**. Mechanisms depicted are dealkylation (S_N2_{NMe}), aliphatic methylene substitution (S_N2_{Aliph}).

In the presented solution studies whereby our samples remain soluble in a medium of reduced dielectric polarity, a more fundamental analysis of the reaction mechanism is fitting where tertiary structural effects such as phase separation are nonexistent. In the simplest definition, benzyl substitution and dealkylation are reactions that proceed via an electron-deficient carbon intermediate. In the ground state, carbon atoms will have a partial positive charge due to the ionic character in the C_α–N^+R_3 bond.[45]

If the amount of positive charge on the α-carbon of the TAA (i.e., benzyl or methyl, or methylene in n-alkyl chains) in the transition state is greater than in the ground state, then substituents which can stabilize the positive charge with through-space *field-* (ion-dipole interaction energy and formal charge), *inductive-* (hyperconjugative electron withdrawal by tetraalkylammonium cation), and/or *resonance* (σ–π bond overlap with benzene ring) *effects* will cause a rate acceleration.[31] However, **pMeBTMA** and **pMeBQA6** are equally affected by these three factors, yet the latter experiences greater degradation.

A study on benzyl leaving groups such as benzyltrialkylammonium salts, in aqueous and non-aqueous solvents, found that hydration numbers significantly increase with longer n-alkyl chain lengths.[46] Hydration is reported to lead to greater stabilization of the associative/dissociative character of the degradation pathway's transition state.[47,48] Additionally, the introduction of a β-carbon capable of extended hyperconjugative donation (i.e., between C_β–$C_\alpha N^+R_3$) as the case with **pMeBQA6**, results in a longer C_{Bn}–N^+R_3 bond that more closely approximates the transition-state structure and facilitates faster solvolytic degradation kinetics.[48–50]

We thus postulate that the observed increase in degradation of **pMeBQA6** compared to **pMeBTMA** results from these solvent effects and a greater polarizable C_{Bn}–N^+R_3 bond. That is, the larger and more structured hydration of the longer n-alkyl chain of the **pMeBQA6** cation likely aids the solubility and stabilization of the electron-deficient benzyl intermediate leading to an increase in the observed degradation over that of **pMeBTMA**.

Consistent with the results of **pMeBTMA** and **pMeBQA6** small molecule analogs, our poly(styrene) sample, **QA6-PS**, experienced a higher loss of its TAA functionality over **BTMA-PS**, albeit at a much higher rate of 92% loss after 3 h at 120 °C, respectively (Figure 4a). Poly(phenylene oxide)-based samples were surprisingly more resistant to alkaline degradation; **BTMA-PPO** lost 66.9% of its TAA groups after 3 hours while **QA6-PPO** was observed to precipitate from solution at 3 h, but yielded a 2 h degradation of 62.9%. Interestingly the increased stability of **BTMA-PPO** over **BTMA-PS** with respective half lives of 120 min and 56.8 min is in distinct contrast with our degradation observations at 80 °C wherein the poly(styrene) derivative (QA-PS) was found to degrade less than its poly(phenylene oxide) analog (QA-PPO) (Figure 4b).[28]

In comparison to our previous work that employed KOD at 80 °C,[26] this study utilizes NaOD at 120 °C and elevated pressures (>13 bar) within our sealed NMR vessel. Temperature and pressure differences can often lead to small but consistent changes in relative kinetic rates. Our observations indicate that structural variation(s) (e.g., activation volumes, transition states, sterics, etc.,)[51] are introduced under our conditions at 120 °C that result in the observed differences in relative rates between PS- and PPO-based samples from those conducted at 80 °C.

Influence of N-Alkyl Interstitial Spacers and Dielectric Effects on Cation Degradation

In both small molecules and polymers, substitution at the benzyl position was the obvious major degradation route. Therefore the effect of interstitial n-alkyl spacers between the aryl ring and the trimethylammonium cation was investigated.

This strategy has shown promise in the literature[36,37] and confirmation of these previous membrane studies with an incisive small molecule measurement was justified.

Pivovar, et al.[29] showed that the background dielectric constant for the benzyl substitution of BTMA has a large effect on the reaction barrier. We observe this dielectric constant effect in our experiments by changing the solvent form pure D_2O to a 3:1 CD_3OD:D_2O mixture. The varying rates of degradation in D_2O and CD_3OD:D_2O can be explained by an analysis of the respective dielectric constants of the solutions. The dielecric constant of the D_2O mixture with NaOD is ~72 at 25 °C and ~42 at 120 °C. This type of solution study is reasonable because the total dielectric constant of a hydrated polymer has been shown to be between 10–30 depending on the water content of the system.[52]

In Figure 5, the alkaline degradation of **ArPrTMA** in pure D_2O and in a 3:1 CD_3OD:D_2O mixture is shown. With the inclusion of a three carbon interstitial spacer, **ArPrTMA**, loses 11.6% of its TAA after 3 h in CD_3OD:D_2O to substitutional displacement (S_N2_{Alibh}) of the trimethylamine and dealkylation (S_N2_{NMe}). In D_2O, **ArPrTMA** degrades 3.3% after 3 h with substitutional displacement of the trimethylamine alone.

When both a three carbon interstitial spacer and a terminal chain are added in the case of **ArPrHxDMA**, an additive effect on the stability is observed as the TAA loss totals just 6.6% from dealkylation alone. In D_2O with NaOD, the degradation of **ArPrHxDMA** is expectedly less yielding a combined 2.7% degradation to substitutional displacement and dealkylation.

The addition of an interstitial n-alkyl spacer has a pronounced effect on the stability of both **ArPrHxDMA** and **ArPrTMA** compounds. For both samples, the removal of an α-C_{Bn} to both a benzene ring and TAA cation, eliminated the pronounced σ–π bond resonance effect that stabilizes the electron-deficient carbon intermediate of the S_N2 reaction as discussed with **pMeBTMA** and **pMeBQA6**. The terminal n-alkyl pendant in **ArPrHxDMA** yielded marginal gains in stability compared to the n-interstitial spacer of **ArPrTMA** alone. The greater effective steric bulk of the n-alkyl pendant of **ArPrHxDMA** likely opposes the close approach of polar solvated nucleophiles leading to marginal gains in stability, but overall the interstitial spacer was observed to have the greatest impact on alkaline stability.

Although not experimentally evaluated in this manuscript, kinetic isotope studies on the elimination reaction (E2) of 2-phenylethyltrimethylammonium ions (i.e., a small molecule containing a two carbon interstitial spacer) was found to lay so far on the side of the products, styrene and trimethylamine, that measuring equilibrium constants at 40 °C in EtO^-/EtOH presented a challenge.[53] This propensity for degradation is not expected in structures containing ≥ 3 carbon interstitial spacers, and thus we recommend this approach for new AEM synthetic designs.

Evidence for Contribution of 1,4-eliminations to Poly(styrene) Analogs

Prior work conducted on self-immolative systems that generate 1,4-quinodimethane analogs[33] invoked the possibility of a parallel mechanism concerning the elimination of trimethylamine in an anion-induced 1,4-elimination on a styrenic small molecule AEM analog. Specifically, we chose to compare **pMeBTMA** that contains a *p*-methyl group that operates as an extension of the π-bond system of the benzene ring in the form of a 1,4-quinodimethane or similarly, an extended hyperconjugated resonance hybrid, to a small molecule without this effect, **ArBTMA**.

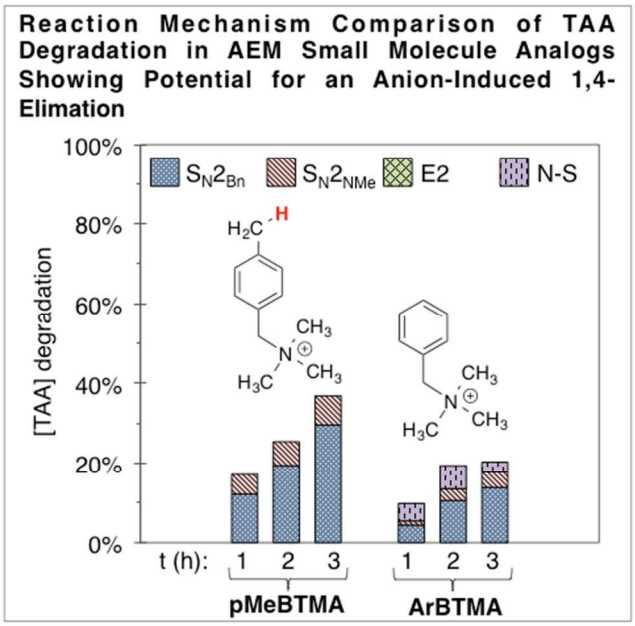

Figure 6. Alkaline degradation of **pMeBTMA** and **ArBTMA** as 30 mM solutions in CD_3OD–D_2O (3:1), 1,4–dioxane (int. std.), and NaOD (20 equiv., 0.6 M) from 0–3 h shown in hourly intervals at 120 °C. Mechanism abbreviations are benzyl substitution (S_N2_{Bn}), dealkylation (S_N2_{NMe}), Hofmann elimination (E2), nonspecific (N–S); the difference in decay between the TAA cation and the sum of observed products.

In Figure 6, the alkaline degradation of **ArBTMA** resulted in a TAA loss of 20.3% after 3 h compared to a significantly higher degradation rate for **pMeBTMA** of 38.6%. This result is intriguing if only the electron-donating properties of a para-methyl group on an aromatic ring are considered. Inductive donation should yield a greater partial negative charge on the benzyl carbon and therefore result in a reduction of electrophilicity. However, when considering the partial positive charge on the benzyl carbon (C_{Bn}) that results from the withdrawing effect of the ammonium, then any substituent that can stabilize the positive charge by resonance or inductive effects will cause a rate acceleration.[45] Distinguishing between the relative contributions of hyperconjugated resonance structures or the formation of intermediates such as the 1,4-quinododimethane that results from anion-induced 1,4-eliminations remains difficult considering that both events result in the products of S_N2_{Bn}.

Studies conducted at 80 °C concluded that **QA-PS** is less susceptible to alkaline degradation than **QA-PPO**,[26] but the opposite trend was observed for **BTMA-PS** and **BTMA-PPO** at 120 °C. Based on these results, we postulate the increase in thermal energy at 120 °C may be sufficient to overcome the energy barrier necessary to activate the 1,4-

elimination mechanism or increase the effects of extended hyperconjugated structures in accelerating the degradation of the corresponding **BTMA-PS** macromolecule.

CONCLUSIONS

In summary, a high temperature ^{1}H NMR-based method to study AEM polymers and analogs under high temperature conditions was introduced that ensures their degradation for meaningful comparisons. The findings indicate that BTMA cations and benzyldimethylammonium analogs with n-alkyl terminal pendants are significantly more susceptible to degradation than TAA cations containing an n-interstitial spacer. Further but minor enhancements in alkaline stability were observed when n-alkyl interstitial and n-alkyl pendant functionalities were combined on a single cation.

The study presented suggests that an AEM poly(phenylene oxide) is more resistant to alkaline degradation at 120 °C than an AEM poly(styrene) polymer; a reversal of stability observed at 80 °C in a previous study. A follow up study with AEM poly(styrene) small molecule analogs suggests that an anion-induced 1,4-elimination degradation mechanism is activated at 120 °C.

These conclusions have potential consequences for BTMA containing poly(styrene)-based polymers in AEMFC high-temperature applications. Although more studies are needed to confirm the findings and given the added stability shown by the addition of the addition of n-alkyl interstitial spacers, it is suggested BTMA-poly(styrene) polymers are replaced with more robust polymer backbones and chemistries are developed for synthesizing AEMs with n-interstitial spacers.

Supporting Information

The Supporting Information is available free of charge via the Internet at http://pubs.acs.org.

Heating block design and ^{1}H NMR degradation spectra of pMeBTMA, QA-PPO, pMeBQA6, QA6-PS, QA-PS, ArBTMA, ArPrTMA, ArPrHxDMA, and QA6-PPO. ^{1}H NMR characterization of pMeBQA6, pMeBTMA, ArPrHxDMA, BTMA-PS, QA6-PS, ArPrTMA, ArBTMA, BTMA-PPO, and QA6-PPO.

Corresponding Author

*E-mail: hickner@matse.psu.edu

Acknowledgments

This work was funded by the Advanced Research Projects Agency – Energy (ARPA-E), U.S. Department of Energy, under award number: DE-AR0000121, the United States-Israel Binational Science Foundation (BSF) through Energy Project no.2011521, and NSF DMREF program under award number CHE-1534326.

References

(1) Fuel Cell Technologies Office. http://energy.gov/eere/fuelcells/fuel-cell-technologies-office (accessed May 22, 2014).
(2) Robertson, N. J.; Kostalik, H. A., IV; Clark, T. J.; Mutolo, P. F.; Abruña, H. D.; Coates, G. W. Tunable High Performance Cross-Linked Alkaline Anion Exchange Membranes for Fuel Cell Applications. *J. Am. Chem. Soc.* **2010**, *132*, 3400–3404.
(3) Varcoe, J. R.; Slade, R. C. T. Prospects for Alkaline Anion-Exchange Membranes in Low Temperature Fuel Cells. *Fuel Cells* **2005**, *5*, 187–200.
(4) Kruusenberg, I.; Matisen, L.; Shah, Q.; Kannan, A. M.; Tammeveski, K. Non-Platinum Cathode Catalysts for Alkaline Membrane Fuel Cells. *Int. J. Hydrogen Energy* **2012**, *37*, 4406–4412.
(5) Piana, M.; Boccia, M.; Filpi, A.; Flammia, E.; Miller, H. A.; Orsini, M.; Salusti, F.; Santiccioli, S.; Ciardelli, F.; Pucci, A. H_2/Air Alkaline Membrane Fuel Cell Performance and Durability, Using Novel Ionomer and Non-Platinum Group Metal Cathode Catalyst. *J. Power Sources* **2010**, *195*, 5875–5881.
(6) Modestov, A. D.; Tarasevich, M. R.; Leykin, A. Y.; Filimonov, V. Y. MEA for Alkaline Direct Ethanol Fuel Cell with Alkali Doped PBI Membrane and Non-Platinum Electrodes. *J. Power Sources* **2009**, *188*, 502–506.
(7) Leng, Y.; Chen, G.; Mendoza, A. J.; Tighe, T. B.; Hickner, M. A.; Wang, C.-Y. Solid-State Water Electrolysis with an Alkaline Membrane. *J. Am. Chem. Soc.* **2012**, *134*, 9054–9057.
(8) Antolini, E. Carbon Supports for Low-Temperature Fuel Cell Catalysts. *Appl. Catal., B* **2009**, *88*, 1–24.
(9) Elezovic, N. R.; Babic, B. M.; Radmilovic, V. R.; Vracar, Lj.M.; Krstajic, N.V, Nb-TiO_2 Supported Platinum Nanocatalyst for Oxygen Reduction Reaction in Alkaline Solutions. *Electrochim. Acta.* **2011**, *56*, 9020–9026.
(10) Kuvernak, A; Smith, B. G., Membrane Electrode Assemblies Based on Porous Silver Electrodes for Alkaline Anion Exchange Membrane Fuel Cells. *Electrochim. Acta.* **2012**, *82*, 284–290.
(11) Merle, G.; Wessling, M.; Nijmeijer, K. Anion Exchange Membranes for Alkaline Fuel Cells: a Review. *J. Membr. Sci.* **2011**, *377*, 1–35.
(12) Uribe, F. A.; Gottesfeld, S.; Zawodzinski, T. A. Effect of Ammonia as Potential Fuel Impurity on Proton Exchange Membrane Fuel Cell Performance. *J. Electrochem. Soc.* **2002**, *149*, A293–A296.
(13) Adams, L. A.; Poynton, S. D.; Tamain, C.; Slade, R. C. T.; Varcoe, J. R. A Carbon Dioxide Tolerant Aqueous-Electrolyte-Free Anion-Exchange Membrane Alkaline Fuel Cell. *ChemSusChem* **2008**, *1*, 79–81.
(14) Deavin, O. I.; Murphy, S.; Ong, A. L.; Poynton, S. D.; Zeng, R.; Herman, H.; Varcoe, J. R. Anion-Exchange Membranes for Alkaline Polymer Electrolyte Fuel Cells: Comparison of Pendent Benzyltrimethylammonium- and Benzylmethylimidazolium-Head-Groups. *Energy Environ. Sci.* **2012**, *5*, 8584–8597.
(15) Page, K. A.; Rowe, B. W. An Overview of Polymer Electrolyte Membranes for Fuel Cell Applications. In *Polymers for Energy Storage and Delivery: Polyelectrolytes for Batteries and Fuel Cells*; ACS Symposium Series; American Chemical Society: Washington, DC, 2012; Vol. 1096, pp 147–164.
(16) Thomas, O. D.; Soo, K. J. W. Y.; Peckham, T. J.; Kulkarni, M. P.; Holdcroft, S. A Stable Hydroxide-Conducting Polymer. *J. Am. Chem. Soc.* **2012**, *134*, 10753–10756.
(17) Price, S. C.; Williams, K. S.; Beyer, F. L. Relationships between Structure and Alkaline Stability of Imidazolium Cations for Fuel Cells. *ACS Macro Lett.* **2014**, *3*, 160–165.
(18) Hugar, K. M.; Kostalik IV, H. A.;Coates, G. W. Imidazolium Cations with Exceptional Alklaine Stability: A Systematic Study of Structure–Stability Relationships. *J. Am. Chem. Soc.*, **2015**, *137*, 8730–8737.
(19) Noonan, K. J. T.; Hugar, K. M.; Kostalik, H. A., IV; Lobkovsky, E. B.; Abruña, H. D.; Coates, G. W. Phosphonium-Functionalized Polyethylene: a New Class of Base-Stable Alkaline Anion Exchange Membranes. *J. Am. Chem. Soc.* **2012**, *134*, 18161–18164.
(20) Zhang, B.; Gu, S.; Wang, J.; Liu, Y.; Herring, A. M.; Yan, Y. Tertiary Sulfonium as a Cationic Functional Group for Hydroxide Exchange Membranes. *RSC Adv.* **2012**, *2*, 12683–12685.

(21) Peterson, J. ^{1}H NMR Analysis of Mixtures Using Internal Standards: a Quantitative Experiment for the Instrumental Analysis Laboratory. *J. Chem. Educ.* **1992**, *69*, 843–845.
(22) Mohanty, A. D.; Bae, C. Mechanistic Analysis of Ammonium Cation Stability for Alkaline Exchange Membrane Fuel Cells. *J. Mater. Chem. A.*, **2014**, *2*, 17314–17320.
(23) Ye, Y.; Elabd, Y. A. Relative Chemical Stability of Imidazolium-Based Alkaline Anion Exchange Polymerized Ionic Liquids. *Macromolecules* **2011**, *44*, 8494–8503.
(24) Arges, C. G.; Ramani, V. Investigation of Cation Degradation in Anion Exchange Membranes Using Multi-Dimensional NMR Spectroscopy. *J. Electrochem. Soc.* **2013**, *160*, F1006–F1021.
(25) Edson, J. B.; Macomber, C. S.; Pivovar, B. S.; Boncella, J. M. Hydroxide Based Decomposition Pathways of Alkyltrimethylammonium Cations. *J. Membr Sci* **2012**, *399–400*, 49–59.
(26) Nuñez, S. A.; Hickner, M. A. Quantitative ^{1}H NMR Analysis of Chemical Stabilities in Anion-Exchange Membranes. *ACS Macro Lett.* **2013**, *2*, 49–52.
(27) Marino, M. G.; Kreuer, K. D. Alkaline Stability of Quaternary Ammonium Cations for Alkaline Fuel Cell Membranes and Ionic Liquids. *ChemSusChem*, **2015**, *8*, 513–523.
(28) Vanecko, J. A.; Wan, H.; West, F. G. Recent Advances in the Stevens Rearrangement of Ammonium Ylides. Application to the Synthesis of Alkaloid Natural Products. *Tetrahedron* **2006**, *62*, 1043–1062.
(29) Chempath, S.; Boncella, J. M.; Pratt, L. R.; Henson, N.; Pivovar, B. S. Density Functional Theory Study of Degradation of Tetraalkylammonium Hydroxides. *J. Phys. Chem. C* **2010**, *114*, 11977–11983.
(30) Ghigo, G.; Cagnina, S.; Maranzana, A.; Tonachini, G. The Mechanism of the Stevens and Sommelet−Hauser Rearrangements. a Theoretical Study. *J. Org. Chem.* **2010**, *75*, 3608–3617.
(31) Anslyn, E. V.; Dougherty, D. A. *Modern Physical Organic Chemistry*; University Science Books, Sausalito, CA 2006.
(32) Errede, L. A. The Chemistry of Xylenes. VIII. the Formation of Spiro-Di-O-Xylylene and Related Compounds. *J. Am. Chem. Soc.* **1961**, *83*, 949–954.
(33) Nuñez, S. A.; Yeung, K.; Fox, N. S.; Phillips, S. T. A Structurally Simple Self-Immolative Reagent that Provides Three Distinct, Simultaneous Responses per Detection Event. *J. Org. Chem.* **2011**, *76*, 10099–10113.
(34) Kreuer, K.-D. Ion Conducting Membranes for Fuel Cells and Other Electrochemical Devices. *Chem. Mater.* **2014**, *26*, 361–380.
(35) Sarode, H. N.; Lindberg, G. E.; Yang, Y.; Felberg, L. E.; Voth, G. A.; Herring, A. M. Insights Into the Transport of Aqueous Quaternary Ammonium Cations: a Combined Experimental and Computational Study. *J. Phys. Chem. B* **2014**, *118*, 1363–1372.
(36) Tomoi, M.; Yamaguchi, K.; Ando, R.; Kantake, Y.; Aosaki, Y.; Kubota, H. Synthesis and Thermal Stability of Novel Anion Exchange Resins with Spacer Chains. *J. Appl. Polym. Sci.* **1997**, *64*, 1161–1167.
(37) Hibbs, M. R. Alkaline Stability of Poly(Phenylene)-Based Anion Exchange Membranes with Various Cations. *J. Polym. Sci. Part B: Polym. Phys.* **2012**, *51*, 1736–1742.
(38) Li, N.; Leng, Y.; Hickner, M. A.; Wang, C.-Y. Highly Stable, Anion Conductive, Comb-Shaped Copolymers for Alkaline Fuel Cells. *J. Am. Chem. Soc.* **2013**, *135*, 10124–10133.
(39) Komokova, E.; Stamatialis, D.; Strathmann, H.; Wessling, M. Anion-Exchange Membranes Containing Diamines: Preparation and Stability in Alkaline Solution. *J. Membr. Sci.* **2004**, *244*, 25–34.
(40) Park, A. M.; Turley, F. E.; Wycisk, R. J.; Pintauro, P. N. Electrospun and Cross-Linked Nanofiber Composite Anion Exchange Membranes. *Macromolecules* **2014**, *47*, 227–235.
(41) Chempath, S.; Einsla, B. R.; Pratt, L. R.; Macomber, C. S.; Boncella, J. M.; Rau, J. A.; Pivovar, B. S. Mechanism of Tetraalkylammonium Headgroup Degradation in Alkaline Fuel Cell Membranes. *J. Phys. Chem. C* **2008**, *112*, 3179–3182.
(42) Deshayes, S.; Kasko, A. M. Polymeric Biomaterials with Engineered Degradation. *J. Polym. Sci. Part A: Polym. Chem.* **2013**, *51*, 3531–3566.
(43) Li, N.; Yan, T.; Li, Z.; Thurn-Albrecht, T.; Binder, W. H. Comb-Shaped Polymers to Enhance Hydroxide Transport in Anion Exchange Membranes. *Energy Environ. Sci.* **2012**, *5*, 7888–7892.
(44) Pan, J.; Chen, C.; Zhuang, L.; Lu, J. Designing Advanced Alkaline Polymer Electrolytes for Fuel Cell Applications. *Acc. Chem. Res.* **2011**, *45*, 473–481.
(45) Streitwieser, A. Solvolytic Displacement Reactions at Saturated Carbon Atoms. *Chem. Rev.* **1956**, *56*, 571–752.
(46) Owens, G.; Guarilloff, P.; Kurucsev, T. Nitrate Selectivity of Ion-Exchange Resins and of Their Model Compounds. II. Viscosity and Density of Benzyltrialkylammonium Salts in Aqueous Solution and ^{14}N N.M.R. Relaxation of the Nitrate Ion. *Aust. J. Chem.*, **1995**, *48*, 1401–1411.
(47) Carey, F. A.; Sundberg, R. J. *Advanced Organic Chemistry: Structure and Mechanisms*; Plenum Publishing Corporation, 2000.
(48) Sunda, A. P.; Mondal, A.; Balasubramanian, S. Atomistic Simulations of Ammonium-Based Protic Ionic Liquids: Steric Effects on Structure, Low Frequency Vibrational Modes and Electrical Conductivity. *Phys. Chem. Chem. Phys.* **2015**, *17*, 4625–4633.
(48) Kenneth C Westaway; Yao-ren Fang; Susanna MacMillar; Olle Matsson; Raymond A Poirier, A.; Islam, S. M. A New Insight Into Using Chlorine Leaving Group and Nucleophile Carbon Kinetic Isotope Effects to Determine Substituent Effects on the Structure of S_N2 Transition States; J. Am. Chem. Soc. **2007**, *111*, 8110–8120.
(49) Harris, J. M.; Shafer, S. G.; Moffatt, J. R.; Becker, A. R. Prediction of S_N2 Transition State Variation by the Use of More O'Ferrall Plots. *J. Am. Chem. Soc.* **2002**, *101*, 3295–3300.
(50) Rastogi, P. P. A Study on Ion-Dipole Interaction Energy of Some Alkali Metal Cations, Halide Anions and Symmetrical Tetraalkylammonium Ions in Different Solvents : Zeitschrift Für Physikalische Chemie. *Z. Phys. Chem.* **1971**, *75*, 202–206.
(51) Eckert, C. A. High Pressure Kinetics in Solution. *Annu. Rev. Phys. Chem.* **1972**, *23*, 239–264.
(52) Kreuer, K. D. On the Development of Proton Conducting Polymer Membranes for Hydrogen and Methanol Fuel Cells. *J. Membr. Sci.* **2001**, *185*, 29–39.
(53) Shanmugam, K.; Subrahmanyam, S.; Subramanian, V. T.; Kodandapani, N.; Stanly, D. F. 2,4-Toluene Diamines—Their Carcinogenicity, Biodegradation, Analytical Techniques and an Approach Towards Development of Biosensors. **2001**, *17*, 1369–1374.

"for Table of Contents use only"

N-Alkyl Interstitial Spacers and Terminal Pendants Influence the Alkaline Stability of Tetraalkylammonium Cations for Anion Exchange Membrane Fuel Cells

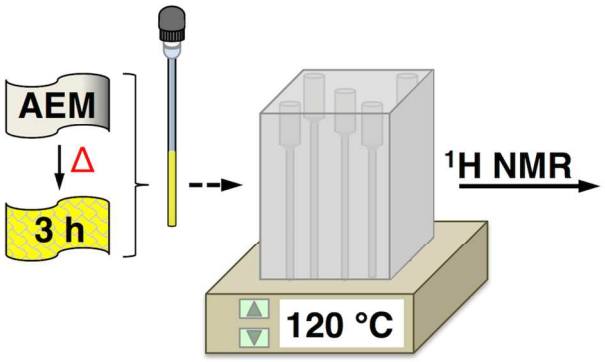
AEM
Δ
3 h
^{1}H NMR
120 °C